LIMNOTEK Perairan Darat Tropis di Indonesia
transforming into Journal Limnology and Water Resources
p-ISSN: 0854-8390 e-ISSN: 2549-8029
https://ejournal.brin.go.id/limnotek

Integrated Field Theoretical Evaluation of Sediment Pond Efficiency in a Tropical Mining Catchment

Bella Koes Paulina Cantik[1], Elenora Gita Alamanda Sapan[2], Ramon Putra[3], Belly Martin[4], Josh Kevin[5]

[1]Faculty of Smart Technology, Civil Engineering Study Program, Universitas Kristen Krida Wacana, Jl. Tanjung Duren Raya West Jakarta, DKI Jakarta 11470, Indonesia.
[2]Research Center for Limnology and Water Resources, National Research and Innovation Agency (BRIN), BJ Habibie Science and Technology Area, South Tangerang, Banten 15314, Indonesia.
[3]Department of Public Housing, Jl. Prof. Dr. Sri Sidewi, Sungai Penuh, Jambi 37152, Indonesia.
[4]PT. Halmahera Persada Lygend (HPAL), Jl. Jendral Sudirman, Central Jakarta, DKI Jakarta 10270, Indonesia.
[5]PT. Leighton Contractors Indonesia, Jl. Ampera Raya, South Jakarta, DKI Jakarta 12550, Indonesia.

Corresponding author's e-mail: bella.paulina@ukrida.ac.id

Received: 29 September 2025; Accepted: 17 November 2025; Published: 20 December 2025

Abstract: Sediment ponds in coal mining operations serve as critical infrastructure for wastewater management. A major challenge in their operation is excessive sediment accumulation, which is often difficult to anticipate accurately, especially when relying solely on theoretical calculations. Such circumstances highlight the importance of an approach that is not solely theoretical, but also considers the actual dynamics observed in the field. The coal mining sediment pond examined in this study was initially constructed to accommodate a catchment area of 205 Ha, with a useful life of 10 years. However, the pond has reached full capacity in less than five years, 53% earlier than expected, indicating the need for re-evaluation, especially as the catchment area is planned to expand to 885 Ha. This study aims to evaluate, compare, and recalculate the sediment pond's capacity under expanded catchment conditions (885 Ha), by integrating field-based measurements and theoretical sediment yield methods to produce a more representative design. The methods employed include the Revised Universal Soil Loss Equation (RUSLE), Lane & Kalinske's Approach, Einstein's Approach, Brook's Approach, and Chang, Simons, and Richardson's Approach. RUSLE utilizes secondary data, while the other methods incorporate both primary and secondary data. The results show a wide range of sediment transport estimates, from 20,184 m^3 using Einstein's to 507,075 m^3 using Chang's. Among the evaluated methods, Lane and Kalinske, as well as Brook, produced sediment volume estimates that closely matched field-based measurements, making them suitable for field conditions. RUSLE produced a lower-bound estimate, while Einstein and Chang's method deviated significantly from the observed range. These findings underscore the importance of integrating field measurements with theoretical models to enhance the reliability of sediment-yield estimation and support informed decision-making in sediment pond.

Keywords: coal mining catchment, sediment pond performance, sediment transport modelling, suspended sediment load

DOI: https://doi.org/10.55981/limnotek.2025.13506

1. Introduction

A substantial proportion of mining operations, particularly coal mining, produce environmentally detrimental effluents commonly referred to as Acid Mine Drainage (AMD). These effluents are typically

characterized by elevated concentrations of heavy metals and other pollutants that degrade water quality and the integrity of aquatic ecosystems integrity (Fahruddin *et al*., 2020; Suryani *et al*., 2022; Saptawartono *et al*., 2024; Syam & Iryani, 2025). AMD is formed through the oxidation of sulfide minerals (most notably pyrite) when exposed to oxygen and water (Saptawartono *et al*., 2024). The aqueous component of this reaction may derive from direct precipitation, subsurface seepage, runoff, and groundwater entering the mining area (Batubara & Saismana, 2019; Noor *et al*., 2021; Siri *et al*., 2022; Nugraha & Isniarno, 2022). Comprehensive analyses of mine-derived effluents have indicated elevated and spatially variable concentrations of contaminants, such as Total Suspended Solids (TSS), iron (Fe), manganese (Mn), and sulfate, underscoring the necessity for site-specific wastewater treatment interventions within mining operations (Wahyudin *et al*., 2021; Syam & Iryani, 2025).

One of the principal mine wastewater management strategies is the implementation of dewatering systems in the form of sedimentation ponds, which are specifically designed to enable the settling of suspended solids, thereby optimizing effluent quality prior to its discharge into receiving water bodies or designated final disposal sites (Murad, 2021; Saputra *et al*., 2023). In Indonesia, this practice is reinforced by regulatory frameworks: the Ministry of Environment and Forestry Regulation No. 5/2022 and Government Regulation No. 22/2021 mandate that mine wastewater must be treated before release to water bodies. Furthermore, the Ministerial Decree of the Ministry of Energy and Mineral Resources No. 1827 K/30/MEM/2018 on Good Mining Practice requires the development of environmental management facilities, including settling ponds, to prevent and mitigate pollution from mining operations. Nevertheless, several studies have indicated that excessive sediment accumulation can pose a significant threat to both the effective storage capacity and the operational lifespan of such facilities, with reported capacity losses ranging from 63% to complete infill relative to the original design specifications (Patro *et al*., 2022).

This case study focuses on a sediment pond associated with coal mining operations in East Kalimantan, Indonesia, observed in 2017. The mining site is segmented into two primary operational zones: the east block, which remains actively operated, and the west block, where extraction activities are nearing completion. The sediment pond evaluated in this study is situated within the east block and was originally engineered with a storage capacity of 445,752 m³ and an anticipated operational lifespan of 10 years. By 2017, however, a performance evaluation was considered necessary due to an expansion of the contributing catchment area from 205 Ha to 885 Ha. The evaluation indicated a marked deviation between the design lifespan and the actual operational lifespan, as evidenced by the complete infilling of sediment across all six compartments of the pond, regardless of initial projections indicating that the pond would reach maximum storage capacity only by 2022.

There are various factors that may cause the actual operational lifespan of a sediment pond to deviate from its design lifespan. One such factor is the inaccuracy in capacity estimation during the planning phase, which can lead to overly optimistic lifespan predictions that do not reflect field conditions. This underscores the need for further comprehensive research to evaluate the storage capacity and performance of sediment ponds. Previous studies have employed theoretical approaches to estimate storage capacity and sediment yield; however, these results should ideally be compiled with empirical data obtained directly from field measurements. The integration of these two approaches can provide a more accurate representation of the reliability of sediment pond design.

Previous studies have examined sediment pond performance in coal mining. Tresnawati *et al*., (2024) evaluated TSS concentrations and deposition volumes in a multi-compartment settling pond, while Febriyanti *et al*., (2024) analyzed treatment capacity based on rainfall-driven inflow dynamics. Putra *et al*. (2021) also assessed the carrying capacity of a settling pond using grab sampling and pollutant load carrying capacity calculations, identifying limited effectiveness across multiple sampling

points. Although these studies underscore the urgency of sediment management, they primarily rely on only empirical observations and do not integrate theoretical sediment transport models. Accordingly, the present study aims to evaluate the performance of a sediment pond by employing theoretical approaches, such as Revised Universal Soil Loss Equation (RUSLE), and those proposed by Lane & Kalinske, Einstein, Brook, and Chang, alongside empirical approaches involving direct sampling at the inlet and outlet of the sediment pond, both after rainfall events and during dry conditions.

2. Materials and Method

This research was conducted as a case study on the useful life of the East Block sediment pond at a coal mining site in East Kalimantan in 2017. Both primary and secondary data were used to support the analysis, including historical rainfall data in 10-year period prior to the study. The method applied in this research was quantitative, combining empirical field measurements and theoretical approaches using the Lane & Kalinske, Einstein, Brook, and Chang equations. The sediment yield estimation in this study focuses on suspended load. The study involved the design and calculation of the sediment pond's storage capacity in response to an increase in the catchment area to 885 hectares. The result for all methods will be compared with the estimated sedimentation deposited based on primary data submitted to the laboratory, as a form of validation of the theoretical approach. The detailed flowchart is illustrated in Figure 1 below.

2.1. Study Area

The research location spans three cities/regencies: Bontang City, Kutai Kartanegara, and Kutai Timur Regency. Bontang City is located in East Kalimantan and is one of the cities that spans between 117°23′ – 117°38′ East longitude and 0°0′ – 0°2′ North latitude. The eastern part has a direct border with the Makassar Strait, while the northern and western parts directly border East Kutai Regency, and the southern boundary meets Kutai Kartanegara Regency. The research area is primarily located in Bontang Selatan Subdistrict, with a small portion extending into Kutai Kartanegara and Kutai Timur Regencies, specifically in the settlement pond area. Bontang Selatan, which is the largest area of Bontang City, covering more than 65% of Bontang's total area, followed by Bontang Utara and Bontang Barat subdistricts. Bontang city is located near the equatorial region, with monthly rainfall ranging between 150-300 mm/month, and an average annual rainfall of approximately 2,500 mm/year (BPS - Statistics of Bontang Municipality, 2022). Bontang City is predominantly covered by forest, shrubland, and mangrove, with settlement areas extending over 20 km² in the northern part. The gently sloping Bontang River flows downward into small islands and wetland areas (Widyasasi *et al.*, 2024). Meanwhile, in Kutai Kartanegara Regency, the Marang Kayu subdistrict covers an area of 866.20 km² and receives an average annual rainfall of approximately 1,800 mm/year. This subdistrict is primarily dominated by forest and plantations, with 28 km² of mining areas, and a small portion of the total area, approximately 9.41 km², serves as settlement and built-up areas. In Kutai Timur Regency, Teluk Pandan subdistrict, located on the southwestern side, has an area of 907 km², accounting for 2.96% of the total area of the regency.

This research is based on a case study of a coal mining site in East Kalimantan. At the time of the study, mining in the west block was nearly completed, while the east block was undergoing large-scale expansion. Currently, the east block remains in operation, making it the active center of mining activities in the area. The location of this research is illustrated in Figure 2.

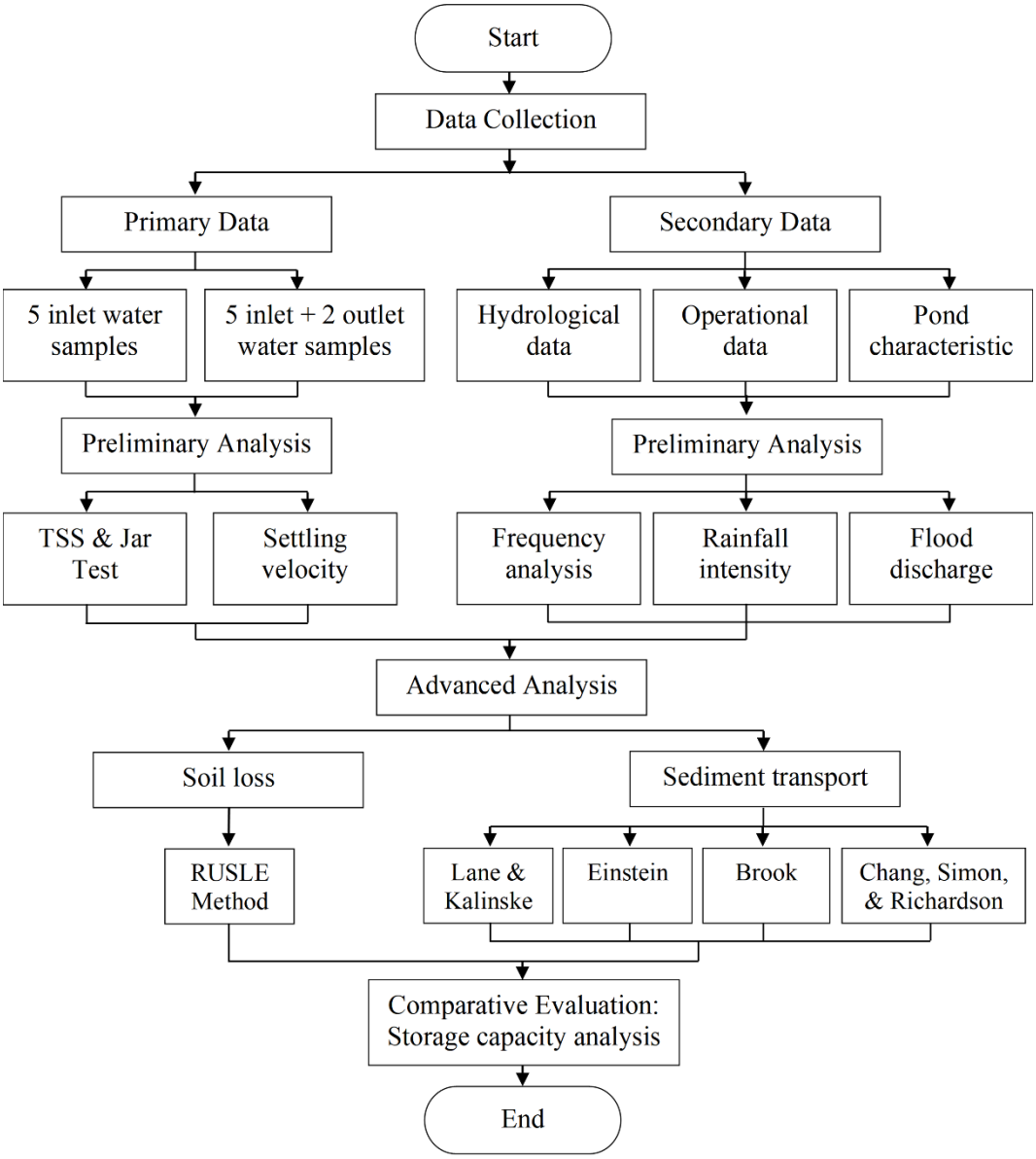

Figure 1. Framework Analysis

Following the site description, the study focuses on the sediment pond used to manage runoff and sediment transport. The catchment area of the sediment pond covers 885 hectares, consisting of four sub-catchment areas, namely waste dump pit 2AN, sump pit 2AN, pit 8AN, and pit 7B, with areas of 205 Ha, 36 Ha, 87 Ha, and 557 Ha, respectively. The existing sediment pond schematic can be illustrated in Figure 3.

2.2. Data Collection

The data used in this study consists of both primary and secondary data. Water sampling refers to SNI 6989.59:2008 on Water and Wastewater — Part 59: Method for Wastewater Sampling. The collection of sediment samples was carried out in two stages: the first was conducted during a period without rainfall, and the second was immediately after the rains. During the dry season, water sampling was limited to the inlet due to minimal or stagnant outlet flow, which was not representative for sediment analysis. The pond's outlet becomes active primarily during rainfall-induced runoff, making inlet sampling more relevant under dry conditions. Water sampling was performed at the inlet of the sediment pond, where five water samples of 500 mL each were collected.

The second stage of sampling, conducted shortly after several hours of rainfall, was carried out at both the inlet and the outlet of the sediment pond, with five water samples taken at the inlet and two water samples taken at the outlet, each of 500 mL in volume.

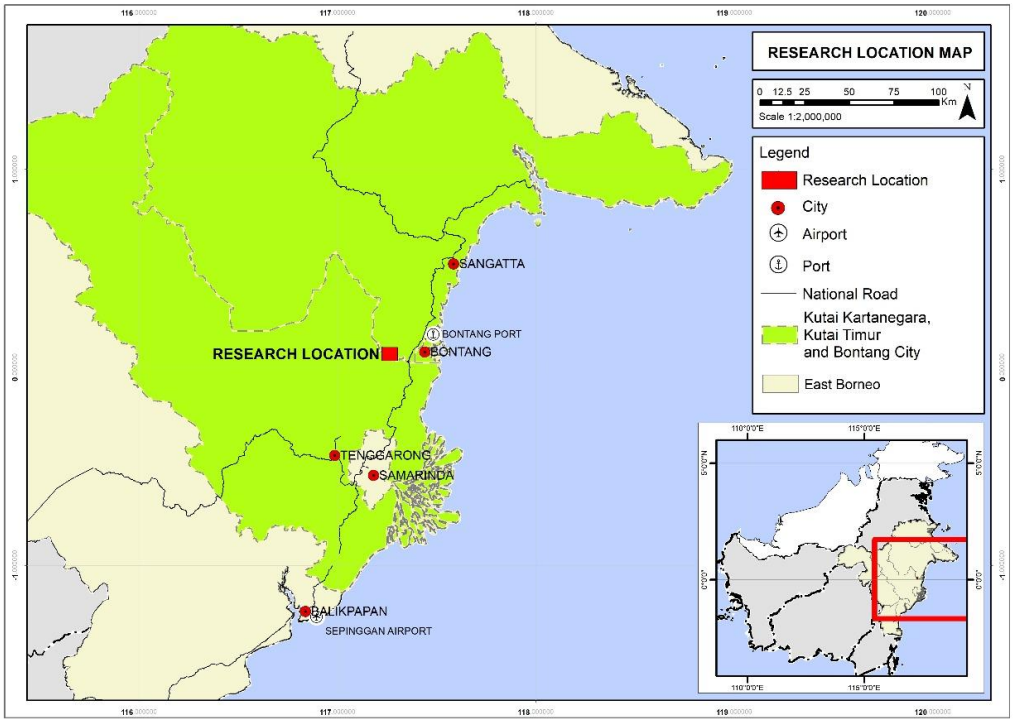

Figure 2. The research location

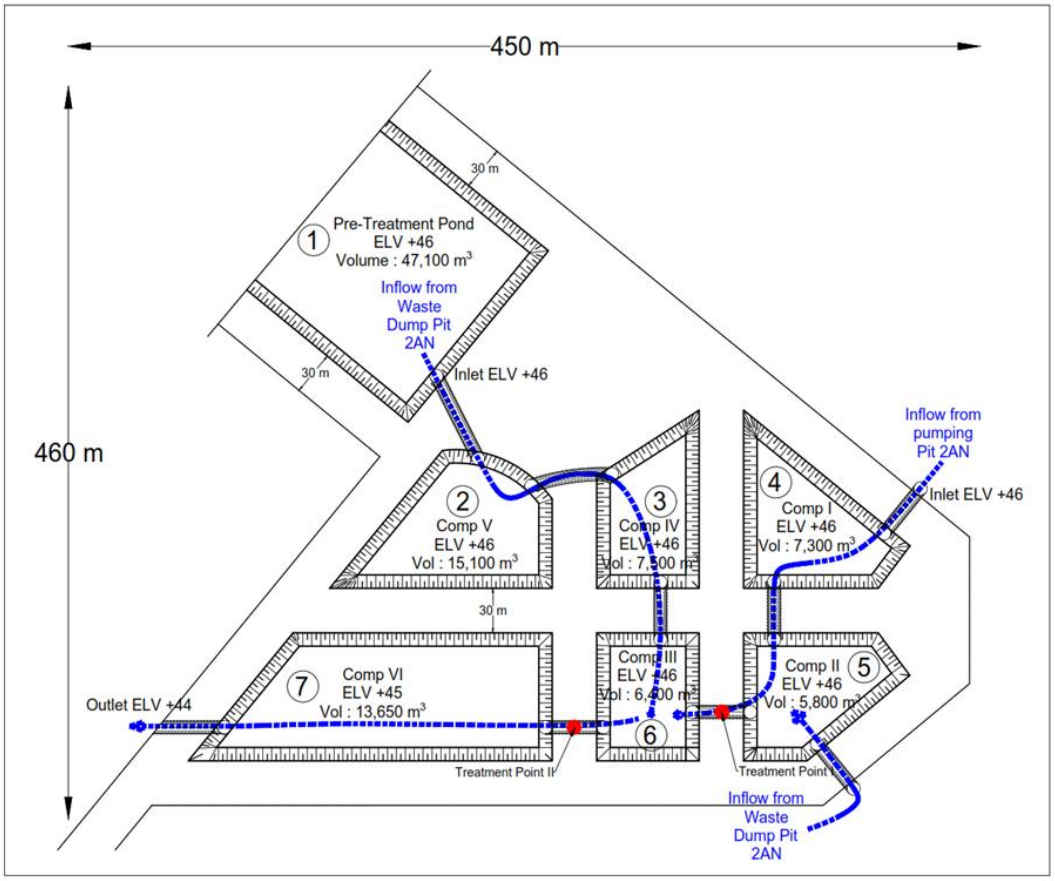

Figure 3. Existing sediment pond schematic

Total Suspended Solids (TSS) and Jar Test analyses were conducted. The TSS test was performed to determine the amount of sediment contained per liter of each sample. The Jar Test, conducted after the TSS analysis, was used to identify the appropriate coagulant dosage required to reduce the TSS concentration in the sediment pond. The TSS and jar test analyses were conducted by the on-site laboratory at the mining location.

The secondary data in this study include maps of Bontang City's administrative boundaries, site locations, and daily rainfall records for the period from 2007 to 2016. Figure 4 below illustrates the maximum daily rainfall. The highest value occurred in 2007, at around 155 mm/day. Moreover, the maximum daily rainfall remained relatively stable from 2008 to 2013. This maximum daily rainfall is analyzed to estimate design rainfall at different return periods.

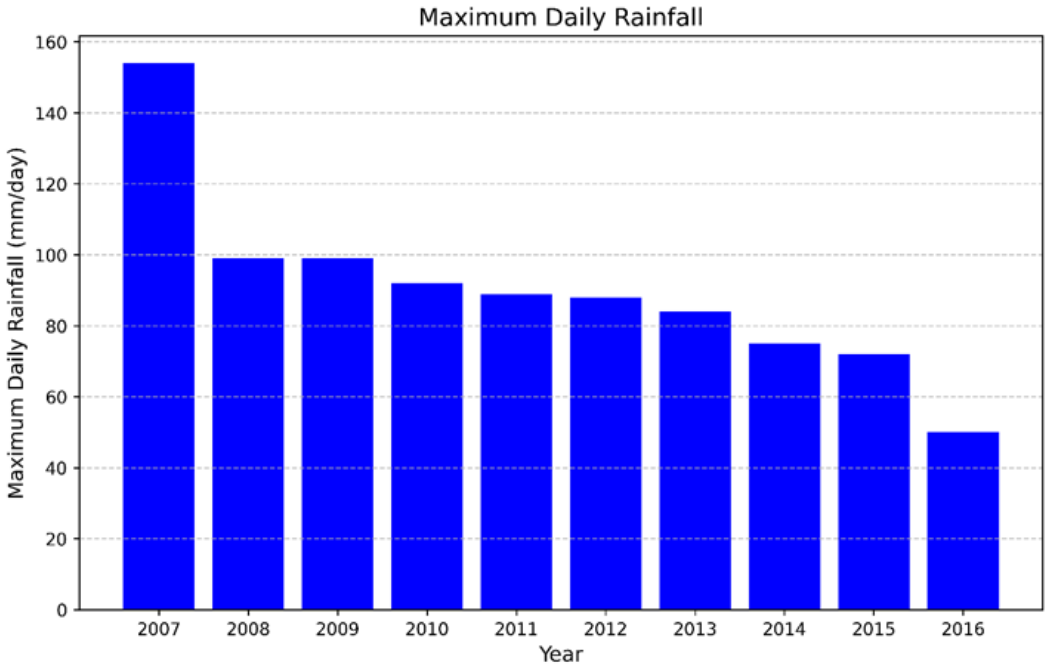

Figure 4. Maximum Daily Rainfall over 10 years

While the numerical data were accessible and sufficient for analysis, the schematic maps of the sub-catchment area's spatial visualizations limited the ability to illustrate catchment boundaries and pond placement. This limitation does not affect the validity of the calculations but should be considered when interpreting the spatial context of the results.

2.3. Design Rainfall and Flood Discharge

In this research, frequency analysis is conducted to identify the relationship between the magnitude of extreme rainfall events and their frequency of occurrence using probability distributions, which is crucial for infrastructure planning (Pudyastuti & Musthofa, 2020; Kalsum *et al.*, 2021). In the context of this research, the value of extreme events refers to the inverse relationship with occurrence probability. For instance, the high flood frequency discharge events are significantly lower than those of moderate or low discharge events. Frequency analysis can estimate the flood discharge or design rainfall for specific return periods, ranging from 1.1 years to 1,000 years, and it can also predict how often floods of a certain magnitude are likely to occur within a given time period (Ginting, 2021; Dwi *et al.*, 2024).

The design rainfall serves as one of the Inputs used to determine rainfall intensity. In this study, the rainfall intensity is calculated using the Mononobe Method. This step is crucial, as flood discharge estimation requires rainfall intensity in millimetres per hour. Through the Mononobe Method, design rainfall data with a daily temporal resolution can be converted into short-duration values (5, 10, 15 … minutes), as presented in Equation 1 (Astarini *et al.*, 2022; Triatmodjo, 2008).

$$I_t = \frac{R_{24}}{24}\left(\frac{24}{t}\right)^{\frac{2}{3}} \quad \text{....Eq.1}$$

where $I_t$is the rainfall intensity for a duration t (mm/h), R_{24} is the maximum 24-hour rainfall (mm), while t is the duration of rain (hours).

In addition, two other parameters are considered in calculating flood discharge using the Ration Method: *A* (the catchment area) and *C* (the runoff coefficient). The catchment area is determined based on the watershed area under study or the area being considered for analysis.

After all necessary parameters for the Rational Method are determined, the flood discharge can be calculated using the Rational Method equation, as presented in Equation 2 (Sari & Irawan, 2021; Triatmodjo, 2008).

$$\mathrm{Q} = 0.278 \times \mathrm{C} \times \mathrm{I} \times \mathrm{A} \quad \text{....Eq.2}$$

where Q is the peak discharge resulting from rainfall with a certain intensity, duration, and frequency (m^3/s), C is the runoff coefficient determined by land cover (dimensionless), I is the hourly rainfall intensity (mm/h), and A is the catchment area (km2).

2.4. Soil Loss by RUSLE Method

The Revised Universal Soil Loss Equation (RUSLE) is one of the methods used to predict the magnitude of erosion or the long-term average annual soil loss caused by rainfall-induced runoff on a given slope (Cantik *et al.*, 2023). The calculation of soil loss using the RUSLE Method is presented in Equation 3.

$$\mathrm{A} = \mathrm{Ri} \times \mathrm{K} \times \mathrm{LS} \times \mathrm{C} \times \mathrm{P} \quad \text{....Eq.3}$$

where *A* represents the average annual soil loss (t/ha/y), *Ri* denotes the rainfall erosivity factor (MJmm/ha/h/y), *K* is the soil erodibility factor (t/ha/h/ha/MJ/mm), *LS* refers to the slop length and steepness factor (dimensionless), *C* is the cover management factor (dimensionless), and *P* represents the support practice factor (dimensionless) (Cantik *et al.*, 2023; Hadi *et al.*, 2023). The calculation of rainfall erosivity is shown in Equation 4 below.

$$\mathrm{Ri} = \sum_{\mathrm{i}=1}^{12} 1.735 \times 10\left(1.5\log_{10}\left(\frac{\mathrm{P_i^2}}{\mathrm{P}}\right) - 0.08188\right) \quad \text{....Eq.4}$$

where *Ri* represents the rainfall erosivity factor (MJmm/ha/h/y), *Pi* denotes the monthly rainfall (mm), and *P* refers to the annual rainfall (mm).

The next parameter is the soil erodibility factor. This factor reflects the soil's resistance to rainfall and surface runoff (Hanifa & Suwardi, 2022) and is determined by soil characteristics such as structure, texture, permeability, and organic matter content (Hanafi & Pamungkas, 2021a; Hanifa & Suwardi, 2022). Another essential parameter to be determined is the slope length and steepness factor (LS), which plays a critical role in the RUSLE model. LS directly influences the rate of erosion and the volume of surface runoff (Hanafi & Pamungkas, 2021b; Pramasela *et al.*, 2022; Faisol *et al.*, 2024).

The following parameter to be determined is the cover management factor (C), which reflects the influence of land cover type on the rate of erosion (Virlayani *et al.*, 2024). A lower C value indicates better land cover performance in reducing erosion, and vice versa. The support practice factor (P) in the RUSLE method represents the effectiveness of soil conservation practices in reducing erosion rates through surface runoff and infiltration management (Sianipar *et al.*, 2023). Compared to the C factor, which focuses on what covers the soil, the P factor emphasizes how the soil is physically managed to resist erosion (Kebede *et al.*, 2021). P values range from 0 to 1, where lower values indicate more effective conservation practices in minimizing erosion (Akbar, 2021; Hanafi & Pamungkas, 2021b; Cantik *et al.*, 2023).

2.5. Settling Velocity Based on Stokes-Newton Law

In the design planning of sedimentation ponds, one of the key parameters that must be analyzed in advance is the particle settling velocity. Several factors influence this velocity, including particle size, fluid type, and viscosity (Omland *et al.*, 2005; Astuti, 2020; Putri *et al.*, 2024). The calculation of particle settling

velocity can be performed analytically based on the physical laws of fluid flow and particle motion within a fluid. For small particles (diameter < 0.1 mm) moving in laminar flow conditions (Reynolds number Re < 1), the settling velocity can be determined using the Stokes–Newton equation (Isnaeni, 2021; Wahyudin *et al.*, 2021) as presented in Equation 5 below.

$$\upsilon_s = \frac{g \times {D_s}^2 \times (\rho_s - \rho)}{18 \times \mu} \quad \text{....Eq.2}$$

where υ_s is the particle settling velocity (m/s), g is the gravitational acceleration (m/s^2), D_S is the diameter of the particle (m), ρ_s is the particle density (kg/m^3), ρ is the fluid density (kg/m3), μ is the fluid viscosity (m^2/s). (Lane & Kalinske 1941; Brooks 1963; Chang *et al.* 1965, as cited in Yang 1996)

2.6. Sediment Yield Methods

The sediment transport rate for the sediment pond was calculated using several analytical approaches as a comparative assessment to the RUSLE method in predicting the pond's storage capacity under a projected catchment area of 885 hectares. The approaches employed in this study include those proposed by Lane and Kalinske, Einstein, Brook, and Chang, Simon, and Richardson. The key differences among these methods in terms of formulation, parameter sensitivity, and theoretical characteristics can be seen in Table 5.

Table 5. Comparative Overview of Sediment Yield Methods

No.	Method	Equation		Sensitivity Parameter	Characteristic
1.	Lane and Kalinske	$q_{sw} = q \times C_a \times P_L \times \exp\left(\frac{15 \times \omega \times a}{U_* \times D}\right)$ $U_* = (g \times D \times S)^{\frac{1}{2}}$	(12) (13)	Flow velocity, particle size, and flow depth	For open channels, integrates hydraulic and particle properties
2.	Einstein	$q_{sw} = 11.6 \times U_* \times C_a \times a \times \left\{\left[2.303 \log \frac{30.2 \times D}{\Delta}\right] I_1 + I_2\right\}$	(14)	Velocity and particle size distribution	Based on velocity-concentration, includes turbulence and lift forces
4.	Brook	$q_{sw} = \frac{q_{sw}}{qC_{md}} \times q \times \gamma \times C_{md}$	(15)	Discharge and sediment concentration	Uses discharge ratio, suitable for design with limited data
5.	Chang. Simon, & Richardson	$q_{sw} = \gamma \times D \times C_a \times \left(VI_1 - \frac{2U_*}{k} I_2\right)$	(16)	Flow geometry and flow velocity	Semi-theoretical, integrates depth and velocity-concentration distribution

Description:
qsw = suspended sediment transport rate (lb/s)
q = total flow discharge per unit width (ft3/s)/ft
Ca = sediment concentration by dry weight (lb/ft3)
PL= flow path coefficient (dimensionless)
ω = settling velocity (in/s)
a = settling height (in, Lane and Kalinske)
a = settling height (ft, Einstein)
U* = horizontal flow velocity (in/s, Lane and Kalinske)
U* = horizontal flow velocity (ft/s, Einstein and Chang)
D = flow depth (in, Lane and Kalinske)
D = flow depth (ft, Einstein and Chang)
Δ = sediment particle characteristic (ft)
I_1 and I_2 = integrals of sediment concentration and flow velocity distribution with respect to flow depth (dimensionless)
qCmd = reference discharge used during sediment concentration measurement (lb/s)/ft
γ = specific weight of water (lb/ft3)
Cmd = dissolved sediment concentration (lb/ft3)
V = low velocity (ft/s)
k = empirical calibration constant (dimensionless)

3. Result and Discussion

3.1. Design Rainfall and Flood Discharge

The frequency analysis conducted in this study processes daily maximum rainfall data recorded over ten years period, from 2007 to 2016. Probability plotting is adjusted according to the number of rainfall data available, after which the calculations of mean, standard deviation, skewness coefficient, and kurtosis coefficient are performed. The statistical parameters calculations of the Frequency Analysis are presented in Table 5 below.

Table 5. Statistical Parameters

No.	Probability (m/(N+1))	Year	Rainfall (mm)
1	0.091	2007	154.00
2	0.182	2008	99.00
3	0.273	2009	99.00
4	0.364	2010	92.00
5	0.455	2011	89.00
6	0.545	2012	88.00
7	0.636	2013	84.00
8	0.727	2014	75.00
9	0.818	2015	72.00
10	0.909	2016	50.11
		The number of data:	10
		Mean:	90.21
		Standard Deviation (S_D):	26.76
		Coeff. Skewness (C_S):	1.35
		Coeff. Kurtosis (C_k):	3.89

Following the calculation of statistical parameters, the rainfall data were evaluated using the Chi-Square Test and the Smirnov-Kolmogorov Test. In the Chi-Square Test, all distributions, including Normal, Log-Normal, Gumbel, and Log-Pearson III, were accepted. Similar results were obtained from the Smirnov-Kolmogorov Test, where all distributions were also accepted. However, according to the Chi-Square Test, the best-fitting distribution was Log-Pearson III, while the Smirnov-Kolmogorov Test indicated Log-Normal as the best fit. Between the two, the higher XT value was selected, which corresponded to the Log-Pearson III distribution. The results of the design rainfall are presented in Table 6. After the Frequency Analysis was carried out, the next step was to calculate the rainfall intensity using the Mononobe method. The results of this calculation are shown in Table 7.

Based on Table 7, the rainfall intensity applied in the Rational Method for flood discharge calculation is taken at a 60-minute duration and a 25-year return period, resulting in 49.978 mm/h. In addition to rainfall intensity, the runoff coefficient is set at 0.3 (undeveloped area). Once all discharge parameters are defined, the flood discharge can be calculated for each catchment area, with detailed results presented in Table 8.

Table 6. Design Rainfall

Probability	Return Period (year)	Design Rainfall (mm)
50%	2	86.614
20%	5	110.314
10%	10	125.463
4%	25	144.163
2%	50	157.850
1%	100	171.377
0%	1000	216.482

Table 7. Rainfall Intensity

Duration (mins)	Return Period (year)						
	2	5	10	25	50	100	1,000
20	62.460	79.550	90.474	103.959	113.829	123.584	156.110
45	36.376	46.329	52.691	60.545	66.293	71.974	90.917
60	30.027	38.244	43.495	49.978	54.723	59.413	75.050
120	18.916	24.092	27.400	31.484	34.474	37.428	47.279

Table 8. Flood Discharge for Each Sub-catchment Area

Sub Catchment Area	A (Ha)	Q (m^3/s)
Waste Dump Pit 2AN	205	8.545
Sump Pit 2AN	36	1.501
Pit 8AN	87	3.626
Pit 7B	557	23.217
Total	**885**	**36.889**

Based on Table 8, the flood discharge for the sediment pond, calculated using the updated catchment area of 885 Ha, is 36.889 m3/s. This flood discharge value is then specifically used as input data in the RUSLE equation and in sediment transport calculations using various analytical approaches. This value represents the actual hydrological condition of the sediment pond's revised catchment area. By incorporating flood discharge based on actual data, the sediment pond design can be calculated more responsively to the potential runoff and sediment load carried during the annual period.

3.2. RUSLE for Soil Loss

Soil loss estimation using the RUSLE method begins with calculating the rainfall erosivity factor, Ri. The value of Ri is derived using Equation 10, which serves as the basis for quantifying rainfall erosivity. The calculated value of Ri from 2008 to 2016 is illustrated in Figure 6 below.

Based on Figure 6, the average annual rainfall erosivity value is 298.161 MJmm/ha/h/y. This value is subsequently used as input in the RUSLE calculation, as RUSLE is specifically designed to estimate annual soil loss. The use of a sufficiently long data period ensures that the results are representative of local climatic conditions and helps to reduce the influence of extreme annual outliers. Following the determination of rainfall erosivity, the LS, C, and P factors are identified by referring to Table 2 – Table 4. The final results of RUSLE-based soil loss estimation are presented in Table 9.

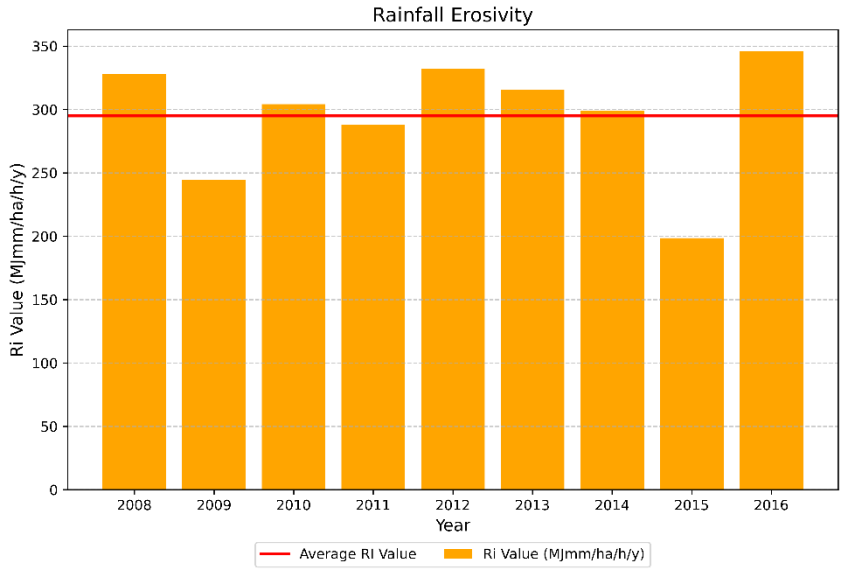

Figure 6. Rainfall erosivity values, Ri

Table 9. Result of RUSLE's Soil Loss

No.	Parameter	Unit	Value	Remarks
1.	Rainfall erosivity (Ri)	MJmm/ha/h/y	298.161	Average rainfall erosivity
2.	Soil erodibility factor (K)	-	0.296	Gray regosol (young, loose soil, commonly found in mining areas)
3.	Slope length and slope steepness factor (LS)	-	1.4	Slope Gradient: 10%
4.	Cover management factor (C)	-	1	Cultivated bare land
5.	Support practice factor (P)	-	1	No conservation practices
	Soil loss by RUSLE (A)	**t/ha/y**	**123.558**	Catchment area of 885 Ha
	Soil loss by RUSLE (A)	**t/y**	**109,349**	

3.3. Settling Velocity by Stokes-Newton Law

The settling velocity of sediment particles in the sediment pond is calculated using the Stokes–Newton Law, as outlined in Equation 11. All parameters required for the settling velocity calculation were obtained directly from laboratory testing of primary data samples, with the exception of the gravitational acceleration value, which is a standardized value. The detailed values used in the calculation are presented in Table 10 below.

Based on the calculations in Table 10, the settling velocity derived from the Stokes–Newton Law is 0.660 m/s or 25.979 in/s. This relatively high settling rate indicates that sediment particles tend to settle quickly under calm flow conditions. Such behaviour supports the effectiveness of the existing sediment pond in facilitating sediment separation.

Table 10. Parameters for settling velocity using Stokes-Newton Law

No.	Parameter Persamaan	Unit	Nilai	Source
1.	Gravitational acceleration (g)	m/s^2	9.81	Standard constant
2.	Particle diameter (Ds)	m	$4x10^{-5}$	
3.	Particle density (ρ_s)	kg/m^3	1,939	Primary sample lab.
4.	Fluid density (ρ)	kg/m^3	1,180	results
5.	Fluid viscosity (μ)	m^2/s	$1{,}003x10^{-6}$	
6.	Settling velocity (υ_s)*	m/s	0.660	Stokes-Newton Law

3.4. Suspended Load Calculation Using Sediment Yield Method

Four analytical approaches were used to estimate suspended sediment load: Lane & Kalinske's Approach, Einstein's Approach, Brook's Approach, and Chang, Simons, and Richardson's Approach. Each method requires a specific set of input parameters to perform the calculation accurately. These parameters include hydraulic characteristics, sediment concentration, flow depth, particle properties, and empirical coefficients. The required parameters for each method are summarized in Table 11.

Based on Figure 7, notable differences are observed in the suspended sediment transport rate (q_{sw}) among the various analytical approaches, indicating that each method exhibits distinct sensitivities to hydraulic parameters and sediment characteristics. The calculation using Einstein's equation yields the lowest sediment transport rate at 0.021 lb/s/ft, reflecting a theoretical approach based on the vertical distribution of velocity and sediment concentration. This method is suitable for controlled flow conditions and very fine particles, but is considered too conservative for sediment pond design in mining areas with high sediment loads.

In contrast, the Brook and Chang, Simons, and Richardson methods produce higher and relatively comparable sediment transport rates (0.433 lb/s/ft and 0.537 lb/s/ft, respectively). Brook's method relies on the ratio of qsw/qcmd and flow velocity correction, while Chang's method incorporates vertical distribution integrals, I_1 and I_2, with a more aggressive correction graph than Einstein's. Both results are deemed suitable for representing dynamic field conditions.

The results of these calculations, along with a comparative analysis of suspended sediment load values across the four methods, are presented in Figure 7. The Lane & Kalinske approach yields a moderate value of 0.245 lb/s/ft, incorporating flow path and sedimentation efficiency through an exponential expression. This method is appropriate when flow discharge and sediment concentration data are well-defined.

Table 11. Parameter Used

No.	Parameter	Unit	Value
1.	Flow discharge per unit width (q)	$(m^3/s)/m$ $(ft^3/s)/ft$	1.230 13.236
2.	Flow depth (R=R'=D)	m in	4 157.48
3.	Sediment concentration (Ca)	lb/ft^3	$6.675x10^{-4}$
4.	Gravitational acceleration (g)	m/s^2 in/s^2	9.81 386.22
5.	Sediment particle size (d65)	in	0.0236
6.	Settling velocity (υ_s)	m/s in/s	0.660 25.979
7.	Settling height (a)	m in	0.271 10.512
8.	Channel slope (S)	-	0.067
9.	Viscosity (μ)	m^2/s in^2/s	$1{,}003x10^{-6}$ $1{,}555x10^{-3}$
10.	Water density (ρ)	kg/m^3 lb/ft^3	1,180 73.667

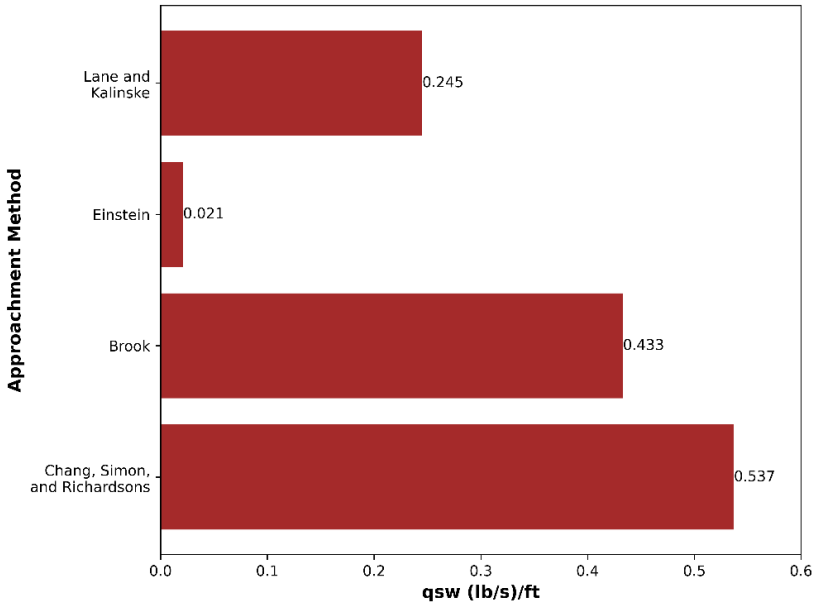

Figure 7. Comparison of suspended load results

3.1 Sediment Pond Design Plan

The sediment pond design plan is calculated based on the total flood discharge and sediment transport values obtained in the previous subsections. This design is derived from the estimated sedimentation that may occur in the pond using five methods: RUSLE, Lane & Kalinske's Approach, Einstein's Approach, Brook's Approach, and Chang, Simons, and Richardson's Approach. The design results for each method are presented in Table 12.

Table 12 presents the result of annual sediment deposition calculated using several methods. Based on the sediment yield's method, annual sediment deposition ranges from 20,184 to 507,075 m^3/year. Pond dimensions were derived by converting daily sediment load into annual volume, then applying a safety factor of 1.3 to ensure adequate capacity under fluctuating sediment loads.

Table 12. Comparison of sediment pond volume results

No.	Sediment deposition (m^3/year)		Pond dimensions (m^3)		
	Method	Results	P (m)	L (m)	d (m)
1	RUSLE	192,063.36	353.33	176.66	4
2	Lane and Kalinske	231,076.18	339.91	169.95	4
3	Einstein	20,183.93	100.46	50.23	4
4	Brook	408,842.15	452.13	226.06	4
5	Chang, Simon, Richardson	507,075.25	503.53	251.76	4

To validate the theoretical calculations, a comparative analysis was conducted using primary data collected from inlet and outlet measurements under existing conditions. The samples were tested in the laboratory for TSS concentration and sedimentation behavior under still water conditions. Based on the test, it was observed that 1.11% to 3.33% of the total water volume settled as sludge, where the lower percentage was observed in samples collected during dry conditions, and the upper bound followed rainfall events. Accordingly, the estimated annual sediment volume ranged from 208,000 m^3/year to 416,100 m^3/year.

When compared to the theoretical calculations presented in Table 12, the estimated annual sediment volume based on laboratory testing (208,000 to 416,100 m^3/year) indicates that the Lane and Kalinske as well as the Brook Methods fall within a relevant range and can be considered a representative approach for field conditions. The RUSLE Method yields a value that is relatively close to the lower bound. In contrast, the Einstein Method produces an estimate significantly below the minimum threshold, while the Chang, Simon, and Richardson exceed the upper bound. Therefore, both require further evaluation regarding the suitability of their parameters and underlying assumptions.

Overall, the result patterns indicate that empirical methods can serve as a baseline, provided that the parameters used are derived from primary data collected and tested directly in the field. Method selection should be further adjusted based on site-specific characteristics, design objectives, and the acceptable level of long-term sedimentation risk.

3.2 Sediment Pond Maintenance Strategies

The variation in estimates of sediment volumes across methods, as shown in Table 12, directly influences the scale and frequency of maintenance required. For instance, methods such as Chang and Brook suggest significantly larger sediment accumulation, which would demand more frequent dredging and larger pond dimensions, while lower estimates may risk underdesign. Therefore, maintenance strategies should be responsive to both theoretical projection and observed field conditions. Several maintenance options can be implemented for the sediment pond, including:

1. Routine Inspection and Monitoring Protocols
   Routine inspection is a cornerstone of sediment pond maintenance in coal mining operations. Regular inspections, especially after heavy rainfall, are essential to assess sediment accumulation, structural integrity, and water quality (Kathuria *et al.*, 1976; Parker & Dumaresq, 2002; Drake & Guo, 2008).
2. Preventive Measures to Minimize Sediment Inflow
   Preventive strategies upstream of sediment ponds can significantly reduce maintenance demands. These include soil stabilization through revegetation, mulching, and erosion control blankets, as well as the installation of check dams and diversion ditches. In Indonesia, best practices for erosion protection during mine development emphasize proactive planning based on hydrological and soil assessments (Sloat & Redden, 2005).
3. Revegetation and Reclamation of Mining Areas
   Revegetation and reclamation are long-term strategies that support sediment

control and ecological restoration. In Indonesia, revegetation practices are guided by forestry science and legal frameworks, with mining companies selecting appropriate plant species to stabilize soil and restore biodiversity. Reclamation efforts typically involve returning topsoil, adding organic matter, and planting fast-growing cover crops (Pambudi *et al*., 2023).

4. Conclusion

The conclusion addressing the objective of this study is that integrating primary and secondary data in formulating the capacity and design of sediment ponds is essential for a representative performance evaluation. This is evident from the significant differences between the RUSLE results and those of sediment yield calculations. Furthermore, the comparison among analytical approaches reveals that sensitivity to field parameters greatly influences the estimation of pond capacity and lifespan. By validating sediment behavior under both dry and post-rainfall conditions, the study demonstrates the value of empirical data in refining theoretical estimates. Future research should focus on dynamic modeling, long-term sedimentation risks, and maintenance strategies to support adaptive and informed decision-making. Through this approach, this study contributes an integrated empirical-theoretical framework applicable to tropical mining environments

Funding Agencies

-

Data availability statement

All data utilized in this study were derived from a real-world case and actual operational activities, obtained directly through field sampling, observation, and technical documentation. However, in accordance with the request of the involved parties, the identity of the institution is not disclosed in this publication to preserve confidentiality and uphold ethical standards of collaboration. Nevertheless, the data used are valid, verified, and available for methodological evaluation within the context of the study.

Author Contributions

BK served as the lead author, conducting field data collection, conceptualizing the overall structure of the manuscript, and drafting the paper. **EG** contributed to hydrological calculations, supervised the analytical process, and assisted in manuscript preparation. **RP** supported the empirical sediment transport analysis, evaluated the computational results, and participated in writing the paper. **BM & JK** provided input on sediment pond maintenance strategies and contributed to the manuscript development.

References

Akbar H. 2021. Prediksi Erosi Dan Teknik Konservasi Tanah Sistem Agroforestri Di Sub Das Krueng Meueh Kabupaten Bener Meriah. *Jurnal Agrium*, 18(2). DOI: https://doi.org/10.29103/agrium.v18i2.5327

Astarini A, Muliadi M, Adriat R. 2022. Studi Perbandingan Metode Penentuan Intensitas Curah Hujan Berdasarkan Karakteristik Curah Hujan Kalimantan Barat. *PRISMA FISIKA*, 10(1), 1. DOI: https://doi.org/10.26418/pf.v10i1.52174

Astuti NI. 2020. Penentuan Viskositas Fluida Dan Kecepatan Terminal Bola Uji Dengan Pendekatan Teori Dan Eksperimen. *Inovasi Fisika Indonesia*, 9(2), 34–40. DOI: https://doi.org/10.26740/ifi.v9n2.p34-40

Batubara MU, Saismana U. 2019. Kajian Teknis Sistem Penyaliran Dan Penirisan Tambang Pit 4 Pt Darma Henwa Site Asam-Asam. Jurnal Himasapta, 2(03). DOI: https://doi.org/10.20527/jhs.v2i03.949

BPS - Statistics of Bontang Municipality. (2022). Bontang Municipality in Figures.

Brooks NH. 1963. Calculation of Suspended Load Discharge from Velocity Concentration Parameters. Proceedings of Federal Interagency Sedimentation Conference.

Cantik, BKP, Putra R, Sapan EGA, Legono D, Afifah KN. 2023. Assessment of Soil Loss Using RUSLE Method in Mrica Reservoir Catchment, Central Java, Indonesia. *LIMNOTEK Perairan Darat Tropis Di Indonesia*. DOI: https://doi.org/10.55981/limnotek.2023.2210

Chang FM, Simons DB, Richardson EV. 1965. Total Bed-Material Discharge in Alluvial Channels. *U.S. Geological Survey Water-Supply Paper* 1498-I.

Drake J, Guo Y. 2008. Maintenance of Wet Stormwater Ponds in Ontario. *Canadian Water Resources Journal*, 33(4), 351–368. DOI: https://doi.org/10.4296/cwrj3304351

Dwi PG, Achmad N, Widyasari T. 2024. Program Analisis Frekuensi Besaran Rancangan Berbasis

Website. *Jurnal Teknik Sipil*, 31(3), 353–360. DOI: https://doi.org/10.5614/jts.2024.31.3.13

Fahruddin F, Haedar N, Abdullah A, Wahab A, & Rifaat R. 2020. Deteksi Unsur Logam Dengan Xrf Dan Analisis Mikroba Pada Limbah Air Asam Tambang Dari Pertambangan Di Lamuru - Kabupaten Bone. *JURNAL GEOCELEBES*, 4(1), 7. DOI: https://doi.org/10.20956/geocelebes.v4i1.7831

Faisol A, Mashudi M, Bachri S. 2024. KOMPARASI NILAI INDEKS FAKTOR PANJANG DAN KEMIRINGAN LERENG PADA BEBERAPA DATA DIGITAL ELEVATION MODEL RESOLUSI MENENGAH. *Jurnal Agritechno*, 18–27. DOI: https://doi.org/10.70124/at.v17i1.1284

Febriyanti S, Riswan R, Arief MZ. 2024. Analisis daya tampung dan kemampuan treatment settling pond berdasarkan data curah hujan di PT Adaro Indonesia. *Jurnal Himasapta*, 8(3), 153. DOI: https://doi.org/10.20527/jhs.v8i3.10835

Ginting S. 2021. Analisis Frekuensi Regional Untuk Data Hujan Harian Maksimum Menggunakan Metode L-Momen. *Akselerasi : Jurnal Ilmiah Teknik Sipil*, 3(1). DOI: https://doi.org/10.37058/aks.v3i1.3556

Hadi F, Syafjanuar TE, Arrahman N, Ramli I. 2023. Nilai Erosi dengan Metode Rusle dari Pemanfaatan Citra Sentinel-2 di Wilayah Sungai Pasee Peusangan. *Jurnal Ilmiah Rekayasa Pertanian Dan Biosistem*, 11(2), 172–187. DOI: https://doi.org/10.29303/jrpb.v11i2.523

Hanafi F, Pamungkas D. 2021a. Aplikasi Model Rusle untuk Estimasi Kehilangan Tanah Bagian Hulu di Sub Das Garang, Jawa Tengah. *Jurnal Geografi : Media Informasi Pengembangan Dan Profesi Kegeografian*, 18(1), 30–36. DOI: https://doi.org/10.15294/jg.v18i1.28079

Hanafi F, Pamungkas D. 2021b. Aplikasi Model Rusle untuk Estimasi Kehilangan Tanah Bagian Hulu di Sub Das Garang, Jawa Tengah. *Jurnal Geografi : Media Informasi Pengembangan Dan Profesi Kegeografian*, 18(1), 30–36. DOI: https://doi.org/10.15294/jg.v18i1.28079

Hanifa H, Suwardi S. 2022. Nilai Erodibilitas Tanah pada Berbagai Penggunaan Lahan dan Tingkat Kemiringan Lahan di Sub Daerah Aliran Sungai Tulis, Banjarnegara, Jawa Tengah. *Biofarm : Jurnal Ilmiah Pertanian*, 18(2), 160. DOI: https://doi.org/10.31941/biofarm.v18i2.2449

Isnaeni M. 2021. Comparison Of Four Particle Deposition Rate Formulae In Laminar Flow. *International Journal of GEOMATE*, 21(84). DOI: https://doi.org/10.21660/2021.84.j2160

Kalsum SU, Gusri L, Dirnasari R. 2021. Analisis Frekuensi Regional Hujan Harian Maksimum Wilayah Sungai Batanghari Menggunakan Metode L-Moment. *Jurnal Civronlit Unbari*, 6(2), 85. DOI: https://doi.org/10.33087/civronlit.v6i2.89

Kathuria DV, Nawrocki, Becker B. 1976. Effectiveness of surface mine sedimentation ponds.

Kebede B, Tsunekawa A, Haregeweyn N, Adgo E, Ebabu K, Meshesha DT, Tsubo M, Masunaga T, Fenta AA. 2021. Determining C- and P-factors of RUSLE for different land uses and management practices across agro-ecologies: case studies from the Upper Blue Nile basin, Ethiopia. *Physical Geography*, 42(2), 160–182. DOI: https://doi.org/10.1080/02723646.2020.1762831

Lane EW, Kalinske AA. 1941. Engineering Calculations of Suspended Sediment. *Transactions of the American Geophysical Union*, 20(3), 603–607.

Murad M. 2021. Rancangan Sump Dan Sediment Pond Bukit 13 Pt. Antam Tbk Ubp Bauksit Tayan Kalimantan Barat. *Jurnal Sains Dan Teknologi: Jurnal Keilmuan Dan Aplikasi Teknologi Industri*, 21(2), 163. DOI: https://doi.org/10.36275/stsp.v21i2.386

Noor MK, Amsah LOMY, Umar EP. 2021. Penanganan Air Limpasan pada Lokasi Penambangan Batubara PT Argo On Star Provinsi Kalimantan Selatan. *Jurnal Geomine*, 8(3), 247. DOI: https://doi.org/10.33536/jg.v8i3.597

Nugraha VK, Isniarno NF. 2022. Analisis Hidrologi untuk Mendukung Rencana Penentuan Temporary Sump pada Tambang Emas. *Jurnal Riset Teknik Pertambangan*, 48–56. DOI: https://doi.org/10.29313/jrtp.v2i1.995

Omland TH, Dahl BD, Saasen A, Svanes K, Amundsen PA. 2005. The influence of particle type and size distribution on viscosity in a nonNewtonian drilling fluid . *ANNUAL TRANSACTIONS OF THE NORDIC RHEOLOGY SOCIETY*, 13(1), 107–110.

Pambudi PA, Utomo SW, Soelarno SW, Takarina N D. 2023. Coal mining reclamation as an environmental recovery effort: a review. *Journal of Degraded and Mining Lands Management*, 10(4), 4811. DOI: https://doi.org/10.15243/jdmlm.2023.104.4811

Parker R, Dumaresq C. 2002. Effluent Characterization, Water Quality Monitoring and Sediment Monitoring in the Metal Mining EEM Program. *Water Quality Research Journal*, 37(1), 219–228. DOI: https://doi.org/10.2166/wqrj.2002.014

Patro ER, De Michele C, Granata G, Biagini C. 2022. Assessment of current reservoir sedimentation rate and storage capacity loss: An Italian overview. *Journal of Environmental*

Management, 320, 115826. DOI: https://doi.org/10.1016/j.jenvman.2022.115826

Pramasela, Limantara LM, Wahyuni S. 2022. Analisis Volume Limpasan Permukaan dan Erosi Tanah dengan Model Soil Conservation Service (SCS) dan Modified Universal Soil Loss Equation (MUSLE) Menggunakan Alat Rainfall Simulator. *Jurnal Teknologi Dan Rekayasa Sumber Daya Air*, 2(1), 410–423.

Pudyastuti PS, Musthofa RA. 2020. Analisa Distribusi Curah Hujan Harian Maksimum di Stasiun Pengukur Hujan Terpilih di Wilayah Klaten Periode 2008-2018. D*inamika Teknik Sipil: Majalah Ilmiah Teknik Sipil*, 13(1), 10–15. DOI: https://doi.org/10.23917/dts.v13i1.11589

Putra SWU, Rahman M, Sofarini D. 2021. Analisis Daya Tampung Settling Pond 02 Terhadap Beban Pencemaran Tss Dari Limbah Tambang Batubara Di Pt Anugerah Lumbung Energi Site Kintap. *Aquatic*, 4(1), 54–62.

Putri MK, Asshaumi RU, Rahmadani NF, Kurnia SI, Mayasari S, Martatino R, Prastowo SHB, Dewi NM. 2024. ANALISIS NILAI KECEPATAN TERHADAP VISKOSITAS PADA FLUIDA. *OPTIKA: Jurnal Pendidikan Fisika*, 8(1), 89–96. DOI: https://doi.org/10.37478/optika.v8i1.3488

Saptawartono, Iashania Y, Murati F, Fidayanti N, Melinda S, & Yakub RI. 2024. PENGELOLAAN DAN PENGENDALIAN AIR ASAM TAMBANG PADA KEGIATAN PERTAMBANGAN BATUBARA. *JURNAL TEKNIK PERTAMBANGAN*, 24(1), 44–51. DOI: https://doi.org/10.36873/jtp.v24i1.11440

Saputra A, Adnyano AAIA, Putra BP, Sutrisno AD, Zamroni A, Machmud A. 2023. A review of Open Channel Design for Mine Dewatering System Based on Environmental Observations. *International Journal of Hydrological and Environmental for Sustainability*, 2(1), 24–31. DOI: https://doi.org/10.58524/ijhes.v2i1.177

Sari NK, Irawan P. 2021. PENERAPAN METODE EMPIRIS DI DAS BATANG LEMBANG UNTUK PERHITUNGAN DEBIT BANJIR RANCANGAN. *Akselerasi : Jurnal Ilmiah Teknik Sipil*, 2(2). DOI: https://doi.org/10.37058/aks.v2i2.2765

Sianipar KO, Sumiyati S, Yulianti NL. 2023. Prediksi Erosi Menggunakan Metode RUSLE pada Lahan Pertanian di Desa Candikuning, Kecamatan Baturiti, Kabupaten Tabanan. *Jurnal BETA (Biosistem Dan Teknik Pertanian)*, 12(1), 80. DOI: https://doi.org/10.24843/JBETA.2024.v12.i01.p09

Siri HT, Widiastuti I, Nusanto G, Amalia Y. 2022. Kajian Teknis Sistem Penyaliran Pada Tambang Batubara Di Pt Banyan Koalindo Lestari, Musi Rawas Utara, Sumatera Selatan. *Jurnal Teknologi Pertambangan*, 7(2), 30. DOI: https://doi.org/10.31315/jtp.v7i2.9118

Sloat MR, Redden R. 2005. Overview of best practices for surface erosion protection and sediment control for the development phase of surface mining for coal in northeast British Columbia.

Suryani MY, Paramita A, Susilo H, & Maharsih IK. 2022. Analisis Penentuan Kadar Besi (Fe) dalam Air Limbah Tambang Batu Bara Menggunakan Spektrofotometer UV-Vis. *Indonesian Journal of Laboratory*, 7. DOI: https://doi.org/10.22146/ijl.v0i0.72451

Syam AN, Iryani AS. 2025. Pengaruh Kegiatan Tambang Terhadap Pencemaran Air : Kajian Terhadap Analisis Air Limbah. *Journal of Scientech Research and Development*, 7(1), 662–673. DOI: https://doi.org/10.56670/jsrd.v7i1.937

Tresnawati N, Asmawi S, Kissinger K, Fauzana NA. 2024. Daya Tampung Settling Pond Terhadap Beban Pencemaran Total Suspended Solid Dari Limbah Batubara Pt. Jorong Barutama Greston. *EnviroScienteae*, 20(2), 220. DOI: https://doi.org/10.20527/es.v20i2.19383

Triatmodjo B. (2008). Hidrologi Terapan. Beta Offset Yogyakarta.

Virlayani A, Bakri S, Indriyanti. 2024. Pengaruh Vegetasi Terhadap Laju Erosi. *Arus Jurnal Sains Dan Teknologi*, 2(2), 606–614. DOI: https://doi.org/10.57250/ajst.v2i2.687

Wahyudin M, Subagiyo L, Sitorus S. 2021. Pengaruh Volume Tampung Kolam Settling pond Terhadap Pengelolaan Air Limbah Pertambangan Batubara di PT. XXX, Kalimantan Timur. *Media Ilmiah Teknik Lingkungan*, 6(1), 1–10. DOI: https://doi.org/10.33084/mitl.v6i1.1398

Widyasasi D, Pramono DA. 2024. Analysis of Mangrove Forest Cover in Bontang City of East Kalimantan Province Using Normalized Difference Vegetation Index. *IOP Conference Series: Earth and Environmental Science*, 1430(1). DOI: https://doi.org/10.1088/1755-1315/1430/1/012020

Yang CT. 1996. Sediment Transport Theory and Practice (B. J. Clark & J. M. Morris, Eds.). The McGraw-Hill Companies, Inc.